

# Au+Au Collisions: the Suppression of High Transverse Momentum in $\pi^0$ Spectra.

D. E. Kahana

31 Pembroke Dr., Stony Brook, NY 11790, USA

S. H. Kahana

Physics Department, Brookhaven National Laboratory  
Upton, NY 11973, USA

(Dated: December 14, 2018)

Au+Au,  $\sqrt{s} = 200$  A GeV measurements at RHIC, obtained with the PHENIX, STAR, PHOBOS and BRAHMS detectors, have all indicated a suppression of production, relative to an appropriately normalized NN level. For central collisions and vanishing pseudo-rapidity these experiments indicate a considerable reduction, relative to that nominally expected from equivalent PP measurements, in charged and particle production, especially at mid- to large transverse momenta. In the PHENIX experiment similar behavior has been reported for  $\pi^0$  spectra. In a recent work [1] on the presumably simpler D+Au interaction, to be considered perhaps as a tune-up for Au+Au, we reported on a hadronic cascade mechanism which can explain the observed moderated  $p_{\perp}$  suppression at higher pseudorapidity as well as the Cronin enhancement at mid-rapidity. Here we present the extension of this work to the more massive ion-ion collisions.

PACS numbers:

## I. INTRODUCTION

The specific question at hand in this work is the suppression of medium to high transverse momentum yields observed in the experimental measurements [2, 3, 4, 5] for Au+Au at 130 GeV and 200 GeV. The experimental results have focused on the  $\eta$  and  $p_{\perp}$ -dependence of the ratio

$$R[AA/NN] = \left( \frac{1}{N_{coll}} \right) \frac{[d^2 N^{ch}/dp_{\perp} d\eta] (AA)}{[d^2 N^{ch}/dp_{\perp} d\eta] (NN)}, \quad (1)$$

where  $N_{coll}$  is a calculated number of binary NN collisions occurring in Au+Au at a designated energy and centrality. One can also, of course, just compare directly to the data without reference to ratios.

The simulation code LUCIFER, developed for high energy heavy-ion collisions has previously been applied to both SPS energies  $\sqrt{s} = (17.2, 20)$  A GeV [6, 7, 8] and to RHIC energies  $\sqrt{s} = (56, 130, 200)$  A GeV [6, 8]. Although nominally intended for dealing with soft, low  $p_T$ , interaction it is possible to introduce high  $p_T$  hadron spectra via the NN inputs, which form the building blocks of the simulations, and to then examine the effect of rescattering, and concomitant energy loss, on such spectra [1]. The simulation is divided into two phase I and II, with all the rescattering and energy loss restricted to the second and considerably reduced energy stage. The first stage sets up the participants, both mesonic and baryonic, their four momenta and positions for the commencement of the cascade in II. The second stage energy loss and interactions within a hadronic fluid play a key role in the eventual suppression of the transverse momentum distribution.

For completeness we present a brief description of the dynamics of this Monte Carlo simulation [1]. Many other simulations of heavy ion collisions exist and these are frequently hybrid in nature, using say string models in the initial state [9, 10, 11, 12, 13, 14, 15, 16] together with final state hadronic collisions, while some codes are purely or partly partonic [17, 18, 19, 20, 21, 22] in nature. Our approach is closest in spirit to that of RQMD and K. Gallmeister, C. Greiner, and Z. Xu [23] as well as work by W. Cassing [9, 23, 24]. Certainly our results seem to parallel those of the latter authors. Both seek to separate initial perhaps parton dominated processes from hadronic interactions occurring at some intermediate but not necessarily late time.

The purpose of describing such high energy collisions without introducing the evident parton nature of hadrons, at least for soft processes, was to set a baseline for judging whether deviations from the simulation measured in experiments existed and could then signal interesting phenomena. The division between soft and hard processes, the latter being in principle described by perturbative QCD, is not necessarily easy to identify in heavy ion data, although many authors believe they have accomplished this within a gluon-saturation configuration [25, 26, 27]. For both D+Au and Au+Au systems we separate the effects of a second stage, a lower energy hadronic cascade, from those of the first stage, a parallel rather than sequential treatment of initial (target)-(projectile) NN interactions.

In the present work, even absent some energy-loss effects which one might anticipate in the initial phase, we do find considerable suppression of the Au+Au transverse momentum spectrum at central rapidity. One might say that the

first stage of our simulation, involving the collective interaction of the initially present nucleons, produces a “hot-gas” of prehadrons which are considerably cooled in an inevitable final state cascade. This cooling constitutes the observed “jet” suppression, not surprisingly a suppression appreciably greater for Au+Au than for D+Au [1, 2]. The second stage II, a true cascade, critically includes energy loss effects. The cascade interactions inevitably soften the initial  $p_{\perp}$  distribution, as II involves considerably reduced energy processes.

## II. THE SIMULATION

### A. Stage I

The first stage I of LUCIFER considers the initial interactions between the separate nucleons in the colliding ions A+B, but is not a cascade. The totality of events involving each projectile particle happen essentially together or one might say in parallel. Neither energy loss nor creation of transverse momentum ( $p_{\perp}$ ) are permitted in stage I, clearly an approximation. A model of NN collisions [6, 7], incorporating most known inclusive cross-section and multiplicity data, guides stage I and sets up the initial conditions for stage II. The two body model, clearly an input to our simulation, is fitted to the elastic, single diffractive (SD) and non-single diffractive (NSD) aspects [28] of high energy  $PP$  collisions [29, 30] and  $P\bar{P}$  data [31]. It is precisely the energy dependence of the cross-sections and multiplicities of the NN input that led to our successful *prediction* [7] of the rather small (13%) increase in  $dN^{ch}/d\eta$  between  $\sqrt{s} = 130$  and  $\sqrt{s} = 200$  A GeV, seen in the PHOBOS data [32].

We find that the addition to stage I baryons of transverse momentum by collision dependent random walk produces in fact a rather ‘hot’ hadronic medium, in effect a strong A-dependent Cronin [33] effect, a medium which is subsequently cooled by the final state cascading collisions in stage II. The comparison of the initial and final  $p_T$  spectra provides an alternative measure of suppression to the above ratio  $R[AA/NN]$ .

A history of the collisions that occur between nucleons as they move along straight lines in stage I is recorded and later used to guide the determination of multiplicity. Collision driven random walk fixes the  $p_{\perp}$  to be ascribed to the baryons at the start of stage II. The overall multiplicity, however, is subject to a modification, based as we believe on natural physical requirements [6].

If a sufficiently hard process, for example Drell-Yan production of a lepton pair at large mass occurred, it would lead to a prompt energy loss in stage I. Hard quarks and gluons could similarly be entered into the particle lists and their parallel progression followed. This has not yet been done. One viewpoint and justification for our approach for hadrons could be to say we attempt to ignore the direct effect of colour on the dynamics, projecting out all states of the combined system possessing colour. In such a situation there should be a duality between quark-gluon or hadronic treatments.

The collective/parallel method of treating many NN collisions between the target and projectile is achieved by defining a group structure for interacting baryons. This is best illustrated by considering a prototypical proton-nucleus (P+A) collision. A group is defined by spatial contiguity. A nucleon at some impact parameter  $b(\bar{x}_{\perp})$  is imagined to collide with a corresponding ‘row’ of nucleons sufficiently close in the transverse direction to the straight line path of the proton, *i. e.* within a distance corresponding to the NN cross-section. In a nucleus-nucleus (A+B) collision this procedure is generalized by making two passes: on the first pass one includes all nucleons from the target which come within the given transverse distance of some initial projectile nucleon, then on the second pass one includes for each target nucleon so chosen, all of those nucleons from the projectile approaching it within the same transverse distance. This totality of mutually colliding nucleons, at more or less equal transverse displacements, constitute a group. The procedure partitions target and projectile nucleons into a set of disjoint interacting groups as well as a set of non-interacting spectators in a manner depending on the overall geometry of the A+B collision. Clearly the largest groups in P+A will, in this way, be formed for small impact parameters  $b$ ; while for the most peripheral collisions the groups will almost always consist of only one colliding NN pair. Similar conclusions hold in the case of A+B collisions.

In stage II of the cascade we treat the entities which rescatter as prehadrons. These prehadrons, both baryonic or mesonic in type, are not the physical hadron resonances or stable particles appearing in the particle data tables, which materialize after hadronisation. Importantly prehadrons are allowed to interact starting at early times, after a short production time [34], nominally the target-projectile crossing time  $T_{AB} \sim 2R_{AB}/\gamma$ . In practice we find that the effective time delay for prehadronic collisions (stage II) is appreciable some 0.2 to 0.4 fm/c in the center of momentum frame. The mesonic prehadrons are imagined to have ( $q\bar{q}$ ) quark content and their interactions are akin to the dipole interactions included in models relying more closely on explicit QCD [34, 35], but are treated here as colourless objects.

Some theoretical evidence for the existence of comparable colourless structures is given by Shuryak and Zahed [36] and by certain lattice gauge studies [37]. In these latter works a basis is established for the persistence of loosely bound

or resonant hadrons above the QCD critical temperature  $T_c$ , indeed to  $T \sim (1.5 - 2.0) \times T_c$ . This implies a persistence to much higher transverse energy densities  $\rho(E) \sim (1.5 - 2.0)^4 \rho_c$ , hence to the early stages of a RHIC collision. Accordingly, we have incorporated into stage II *hadron sized* cross-sections for the interactions of these prehadrons, although early on it may in fact be difficult to distinguish their colour content. Such larger cross-sections indeed appear to be necessary for the explanation of the apparently large elliptical flow parameter  $\nu_2$  found in measurements [38, 39].

The prehadrons, which when mesonic may consist of a spatially close, loosely correlated quark and anti-quark pair, are given a mass spectrum between  $m_\pi$  and 1.2 GeV, with correspondingly higher upper and lower limits allowed for prehadrons including strange quarks. The Monte-Carlo selection of masses is then governed by a Gaussian distribution,

$$P(m) = \exp(-(m - m_0)^2/w^2), \quad (2)$$

with  $m_0$  a selected center for the prehadron mass distribution and  $w = m_0/4$  the width. For non-strange mesonic prehadrons  $m_0 \sim 800$  MeV, and for strange  $m_0 \sim 950$  MeV. Small changes in  $m_0$  and  $w$  have little effect since the code is constrained to fit hadron-hadron, data.

Too high an upper limit for  $m_0$  would destroy the soft nature expected for most prehadron interactions when they finally decay into ‘stable’ mesons. The same proviso can be put in place for prebaryons, restricting these to a mass spectrum from  $m_N$  to 2 GeV. However, in the present calculation the prebaryons are for simplicity taken just to be the normal baryons. The mesonic prehadrons have isospin structure corresponding to  $\rho$ ,  $\omega$ , or  $K^*$ , while the baryons range across the octet and decuplet.

Creating these intermediate degrees of freedom at the end of stage I simply allows the original nucleons to distribute their initial energy-momentum across a larger basis of states or Fock space, just as is done in string models, or for that matter in partonic cascade models. Eventually, of course, these intermediate objects decay into physical hadrons and for that purpose we assign a uniform decay width  $\sim \Gamma_f$ , which then plays the role of a hadronisation or formation time,  $1/\Gamma_f \sim 1fm/c$ .

## B. Elementary Hadron-Hadron Model

The underlying NN interaction structure involved in I has been introduced in a fashion dictated by standard proton-proton modeling [28]. A division is made into elastic, single diffractive (SD) and non-single diffractive components. Fits are obtained to the existing two-nucleon data over a broad range of energies  $\sqrt{s}$ , using the same prehadrons introduced above. No rescattering, only decay of these intermediate structures is permitted in the purely NN calculation. Specifically the meson-meson interactions are scaled to 4/9 of the known NN cross-sections, thus no new parameters are invoked. Indeed, since only known data then constrains the prehadronic interaction, this approach is a parameter-free input to the AA dynamics.

## C. Groups

Energy loss and multiplicity in each group of nucleons is estimated from the straight line collision history recorded in stage I. To repeat, transverse momentum of prebaryons is assigned by a random walk having a number of steps equal to the number of collisions suffered. The multiplicity of mesonic prehadrons cannot be similarly directly estimated from the number of NN collisions in a group. We argue [40] that only spatial densities of generic prehadrons [6, 7] below some maximum are allowable, *viz.* the prehadrons must not overlap spatially at the beginning of stage II of the cascade. The prehadrons then constitute an incompressible fluid.

The KNO scaled multiplicity distributions, present in our NN modeling are sufficiently long-tailed that imposing such a restriction on overall multiplicity can for larger nuclei affect results even in P+A or D+A systems. In earlier work [6, 8] the centrality dependence of  $dN/d\eta$  distributions for RHIC energy Au+Au collisions was well described with such a density limitation on the prehadrons, which was not carried out as efficaciously as in the present work, especially with respect to highly peripheral collision.

Again, importantly, the cross-sections in prehadronic collisions were assumed to be the same size as hadronic, *e. g.* meson-baryon or meson-meson values *etc.*, at the same center of mass energy, thus introducing no additional free parameters into the model. Where the latter cross-sections or their energy dependences are inadequately known we employed straightforward quark counting to estimate the scale. In both SPS, Pb+Pb and RHIC Au+Au events at several energies it was sufficient in earlier works to impose this constraint at a single energy. In the present modelling the densities are actually estimated internally and thereby restricted dynamically. The inherent energy dependence in the KNO-scaled multiplicities of the NN inputs and the geometry then take over.

### D. High Transverse Momenta

One question which has yet to be addressed concerns the high  $p_\perp$  tails included in our calculations. In principle, LUCIFER is applicable to soft processes *i. e.* at low transverse momentum. Where the cutoff in  $p_\perp$  occurs is not readily apparent. In any case we can include high  $p_\perp$  meson events through inclusion in the basic hadron-hadron interaction which is of course an input rather than a result of our simulation. Thus in Fig(1) we display the NSD  $(1/2\pi p_\perp)(d^2 N^{charged}/dp_\perp d\eta)$  from UA1 [30]. One can use a single exponential together with a power-law tail in  $p_\perp$ , or alternatively two exponentials, to achieve a fit of the output in PP to UA1  $\sqrt{s}=200$  GeV data. A sampling function of the form

$$f = p_\perp (a \exp(-p_\perp/w) + b/((1 + (r/\alpha)^\beta)), \quad (3)$$

gives a satisfactory fit to the PP data in the Monte-Carlo.

Additionally, since we, for the moment, constrain our comparisons to the production of neutral pions in Au+Au we also present, in Fig.(2) the PHENIX [41] midrapidity  $p_\perp$  yield for NN together with our representation of this spectrum. These NN generated  $p_\perp$  spectra, inserted into the code, were first applied to the meson  $p_\perp$  distribution in D+Au [1] and now of course to Au+Au. No correction is made for possible energy loss in stage I, an assumption parallel to that made by the BRAHMS and all other RHIC experiments, in analysing  $p_\perp$  spectra and multiplicities irrespective of low or high values. However, some explicit energy loss is definitely present in the collisions of stage II, in the dynamics through energy conservation and by a modification of the  $p_\perp$  spectra with energy.

Since we impose energy-momentum conservation in each group, a high  $p_\perp$  particle having say, several GeV/c of transverse momentum, must be accompanied in the opposite transverse direction by one or several compensating mesons. Such high- $p_\perp$  leading particles are not exactly jets, to the extent that they did not originate in our simulation from hard parton-parton collisions, but they yield much of the same observable experimental behaviour. It must be emphasized that the totality of  $p_\perp$  events is small, certainly for the NN collisions seen in Figs.(1,2)) and also as we will see for any AA events. In fact some 90% of all final mesonic yields occurs for  $p_\perp \leq 0.7$ . This implies that our treatment of such high  $p_\perp$  processes is indeed a perturbation, unlikely to alter the overall dynamics. The simulation definitely treats hard processes, if only through the observed behaviour in NN over a range of energy.

We note that the second phase (II) is truly a much softer cascade with the collisions between prehadrons, for example, involving energies less than  $s^{1/2} \sim 15$  GeV and even lower averages. These energy levels in II were arrived at by sharing of energy-momentum in the original baryon groups with the produced mesonic prehadrons. Since much of the physics here results from stage II of the simulation it is permissible to use soft physics as a driving force in the overall dynamics.

That the high  $p_\perp$  prehadrons produced should be given hadronic-like cross-sections perhaps requires some justification. We offer two possibilities. Molnar [38] has tried to correct the 'flow' deficiencies of partonic cascades by introducing coalescence of quark-like partons at an early stage in the cascade. Clearly such coalescence probabilities will decrease steeply with increasing transverse momentum, at say small rapidity, but that is just what is observed in the meson production from both PP and AA. We then argue that the coalescence probability will be greatest for the larger transverse-sized mesons produced and such objects will dominate the dynamics.

Furthermore, and actually relevant to our specific simulation, the earliest meson-meson collisions in our second stage cascade II have a first peak in time at some .25-.35 fm/c while in fact collisions extend to considerably later time. This permits even smaller prehadrons to have appreciably increased their transverse size before collision and simultaneously suggests most collisions are between comovers. Also, the premesons, which dominate the second stage dynamics, are given only 4/9 the total cross-section of baryon-baryon and hence need only possess considerably reduced effective transverse sizes, than say baryons.

### E. Initial Conditions for II

The final operation in stage I is to set the initial conditions for the hadronic cascade in stage II. The energy-momentum taken from the initial baryons and shared among the produced prehadrons is established and an upper limit placed on the production multiplicity of prehadrons and normal hadrons. A final accounting of energy sharing is carried out through an overall 4-momentum conservation requirement. We emphasize that this is carried out separately within each group of interacting nucleons.

The spatial positioning of the particles at this time could be accomplished in a variety of ways. We have chosen to place the prehadrons from each group inside a cylinder, for a A+B collision, given the initial longitudinal size of the interaction region at each impact parameter. We then allow the cylinder to evolve freely according to the longitudinal momentum distributions, for a fixed time  $\tau_p$ , defined in the rest frame of each group. At the end of  $\tau_p$  the total

multiplicity of the prehadrons is limited so that, if given normal hadronic sizes appropriate to meson-meson cross-sections  $\sim (2/3)(4\pi/3)(0.6)^3 \text{ fm}^3$ , they do not overlap within the cylinder. Such a limitation in density is consonant with the general notion that produced hadrons can only exist when separated from the interaction region in which they are generated [40]. One can conclude from this that the prehadron matter acts like an incompressible fluid, viz. a liquid, a state described in the earliest calculations with LUCIFER [1, 6].

Up to this point longitudinal boost invariance is completely preserved since stage I is carried out using straight line paths. The technique of defining the evolution time in the group rest frame is essential to minimizing residual frame dependence which inevitably arises in any cascade, hadronic or partonic, when transverse momentum is present. This is due to the finite size of the colliding objects implied by their non-zero interaction cross-section.

The collision history recorded enumerates the number of interactions suffered by any baryon group member and allows us to assign a transverse momentum through random walk. The premesonic multiplicities, subject to the maximum density injunction, are obtained using the KNO scaling we invoke for the elementary NN interactions and the known dependence on flavour. The production of baryon-antibaryon pairs is allowed, guided again by NN constraints. Transverse momentum is generated for the prehadrons and other produced particles, paying attention to the random walk increase for mesons created by multiple baryon-baryon collisions. Finally, overall energy-momentum conservation is imposed and with it the multi-particle phase space defined.

### III. STAGE II: FINAL STATE CASCADE

Stage II is as stated a straightforward cascade in which the prehadronic resonances interact and decay as do any normal hadrons present or produced during this cascade. Appreciable energy having been finally transferred to the produced particles these ‘final state’ interactions occur at considerably lower energy than the initial nucleon-nucleon collisions of stage I. This cascade of course imposes energy-momentum conservation at the two body collisional level and leads to additional transverse momentum production. For Au+Au, the effect of prehadron-prehadron interaction is truly appreciable, greatly increasing multiplicities and total transverse energy,  $E_\perp$  through both production and eventual decay into the stable meson species. But also, as we will see, in the suppression of high  $p_\perp$  production.

We are then in a position to present results for Au+Au 200 GeV collisions. These appear in Figs(3–7) for various double differential transverse momenta spectra or their derivative ratios. Most contain comparisons with PHENIX [4, 41]  $\pi^0$  measurements. In future work we consider also charged data, but there produced proton spectra play an increasingly larger role with increasing  $p_\perp$ . One expects similar global behaviour.

The initial conditions created to start the final cascade could have perhaps been arrived at through more traditional, perhaps partonic, means. The second stage would then still proceed as it does here. We reiterate that our purpose has been to understand to what extent the results seen in Figures (1-7) are affected by stages I and II separately. *i. e.* do they arise from initial or from final state interactions.

### IV. RESULTS: COMPARISON WITH $\pi^0$ DATA

Figs. (1) and (2) speak to the input nucleon-nucleon data and this elementary production of  $\pi^0$ 's and charged particles. These transverse momentum spectra at mid-rapidity have been compared to results from PHENIX [41] and UA1 [30]. Fig(3) contains the simulated  $\pi^0$  transverse momenta spectrum for Au+Au at  $\eta = 0$  alongside the PHENIX data [4]. To a large extent the suppression observed experimentally is paralleled by the simulated calculations. The production time  $\tau_p$  introduced above was given two values ( $2R_{Au}/\Gamma_{average}$ ) and twice this value. The variation with this initial state time, a parameter in our modeling, was small. The  $\Gamma$ 's here are the longitudinal Lorentz factor defined above and introduced for each baryon group separately in its rest frame. For the symmetric Au+Au collision this change of time is only of small consequence for minimising frame dependence.

What conclusions are to be drawn from these first results? Most definitely, one cannot ignore final state cascading. Moreover, for the assumptions we have made, the most crucial being the perhaps early commencement of such cascading, the suppression cannot be considered as necessarily a sign for production of a quark-gluon plasma: perhaps only a prehadron dominated medium after some initial delay. We repeat: despite the apparently short time  $\tau_p$  at say  $\sqrt{s} = 200 \text{ GeV}$ , one finds in practice that the second stage collisions have an effective production or delay time of  $0.25 - 0.35 \text{ fm/c}$  and continue for some tens of fermis/c. Thus ‘comoving’ collisions likely dominate the cascade. Since the pQCD approach is clearly more fundamental, provided a clear treatment of soft processes can be included, one cannot rule it out as a basis for interpretation. But surely it is interesting to pursue an alternative, albeit more phenomenological, nuclear-system oriented view. A view which simply suggests that more detailed and definite signs of QCD plasma must be sought, especially from the earliest times in the ion-ion collision.

It is instructive to deconstruct the elements of the simulation, i.e. to separate the spectrum at the conclusion of I from that resulting from both I+II. In Fig.(4) the  $\pi^0$  transverse momentum yield is shown for both these cases against the experimental data. It is immediately evident that the many virtual NN collisions in stage I produce a much elevated  $p_\perp$  output and that this is in turn reduced by more than an order of magnitude by collisions with presumably other prehadrons in II. Part of this effect is through inclusion in the dynamics of at least a kinematical treatment of energy loss. Thus the above analogy of an initial hot gas cooled by final state interactions during expansion, is apt.

One might well turn this around and declare that the final state scattering of a given prehadron with comovers has cut down the Cronin effect, a reduction which suggests the applicability of the term ‘jet suppression’ through final state interactions. One notes parenthetically that particles lost at high  $p_\perp$  are compensated for by an increase at the lowest  $p_\perp$ ’s. This is of course part of the effective cooling observed.

A second and equally important criterion for the simulation is the maximum densities created as initial conditions for II. Fig(5) cast some light on this and on another issue, the actual transverse energy density attributed to the earliest stages of the collision. We have included in this figure the charged  $dN/d\eta$  spectra, including a BRAHMS charged meson result (compared to a simple fit):

- (a) for the totality of ‘stable’ mesons in I+II,
- (b) the same result for I alone when only decays of prehadrons but no stage II reinteractions are permitted,
- (c) and finally for the prehadrons in I only, with no decays.

It is evident that some 2/3 of the summed transverse energy  $E_\perp$  is generated in the second expanding phase II when the system is increasing both longitudinally and transversely. The initial, very early,  $E_\perp$  generated is then reduced commensurably, falls well below the Bjorken limit and is hence not all available for initial ‘plasma’ generation. In present calculations at the initialisation of II, and keeping in mind the average masses assigned to prehadrons centered at 0.8 to 1.0 GeV, the ambient transverse energy densities are  $\leq 1.8 \text{ GeV}/fm^3$  for the shortest initial time  $\tau_p$  chosen and correspondingly less for longer times.

It is also clear that the density of prehadrons, each of which in I as seen from Fig.(5) decays into some 2.5 stable hadrons. The rather lengthy decay time assigned,  $\tau_f \sim 1 \text{ fm}/c$ , ensures that the stable species enter only sparingly in the dynamics of II. Thus the bugbear of over-scattering or over-cascading is reduced to manageable proportion. The initial limit on density is of course an additional key element.

### A. Ratios of Au+Au to NN Production

In Fig.(6) we display the oft-quoted ratio [2, 3, 5, 43] introduced in Eqn.(1). The discrepancies between simulation and data are magnified but the general effect of agreement shown in Fig.(3) is left intact. The direct double-differential cross-sections fall many orders of magnitude over the reported range but the ratios to normalized proton-proton cover a much compressed range over the reported  $p_\perp$  interval. We have in this figure presented PHENIX  $\pi^0$  data from an early paper [4], but more recent data [44] tells a somewhat modified tale. The dip in  $R_{AuAu/NN}$  at the lowest transverse momentum point  $p_\perp = 1.25 \text{ GeV}/c$ , implying a maximum in this ratio at a bit higher  $p_\perp$ , has apparently disappeared. This is so for both the 0–5% and 0–10% data resulting in curves more in accord with the corresponding theoretical calculations. The equivalent charged ratios [2, 3, 5, 43] do exhibit this apparent maximum but in a region where the proton spectra show considerable activity. One might also question the use of the ratio  $R_{AA/NN}$  at very low  $p_\perp$ , involving as it does the number of binary collisions. A relevant or preferred divisor there might be the number of participants.

In Fig.(6) we present LUCIFER results for 0% – 10% centrality, but the shape is generic at least for reasonably central collisions. As one approaches extreme peripherality the ratio will at all  $p_\perp$  eventually approach unity, provided of course the number of binary collisions  $N_{coll}$  is also adjusted.

It must be emphasized that  $R_{AuAu/NN}$  is quite sensitive to the invariant  $PP$  cross-section. We have prepared both theoretical and experimental ratios using the PHENIX experimental  $PP$  values, indeed using our own constructed fits to the latter data and for smoothness to the simulated  $Au + Au$ . The fit to PHENIX  $PP$  is shown in Fig.7. It should be again noted that the prehadron-liquid modeling employed here is to be considered somewhat metaphorically and that no additional parameters, over and above the times for production,  $\tau_p$ , and hadronisation (decay of prehadrons),  $\tau_f$ , were made available for sculpting the data, nor would such editorializing be sensible. We seek only a qualitative and reasonably quantitative understanding of the observations.

The simulations performed here overestimate, but not by much, the suppression of the spectrum at the lowest  $p_\perp$ , but yield an overall, perhaps surprisingly, accurate description.

## V. CONCLUSIONS

Repeating: an alternative reading of the high transverse momentum suppression has been presented. It is hard to conclude definitively from what is presented here that the standard pQCD + some soft process treatment is not still a more fundamental approach. But at question is just this coupling to soft processes, not unrelated to possible early appearance of an excitation spectrum of hadronic-like structures. The latter, if generated sufficiently early may alter the role of soft processes even on high  $p_{\perp}$  objects passing through a much more dense cloud of soft prehadronic. It is fact just the nature of the soft processes which is at question. Certainly there is still a silent elephant lurking in the dynamics: the observation of rather large elliptical flow in the meson spectrum [39]. These flow measurements are most easily reproduced theoretically if hadronic-sized cross-sections are invoked [38].

In the work on D+Au [1] the use of such a prehadronic spectrum exposed most clearly the simple role of dynamically-driven geometry in ratios of BRAHMS  $p_{\perp}$  spectra at varying pseudorapidity. In D+Au high  $\eta$  charged production, with attendant higher energies for produced particles, results mostly from nucleon-nucleon collisions in a ring around the periphery of the target, at a reduced frequency in comparison to  $\eta=0$ , essentially a volume process. Hence the  $\sim 2$  suppression seen in BRAHMS [2] for  $\eta = 3.2$  yield relative to  $\eta = 0$ . For Au+Au the degradation in  $p_{\perp}$  spectra in the phase II cascade is considerably increased and suppression, when appropriately to NN, is seen even for  $\eta = 0$ . Certainly, the RHIC experiments are probing unusual nuclear matter, at high hadronic and energy density, in exciting terms and more experimental exploration is required.

It would seem, however, that a direct attempt at a pQCD explanation of this behaviour must claim that, at the very least, all soft mesons are produced in essentially hard collisions. The presentation here provides an interesting case for relying on the geometry of soft, low  $p_{\perp}$ , processes, essentially mirrored in hard processes, to produce the major features of the D+Au and Au+Au data. True enough, the high  $p_{\perp}$  tails in distributions are merely tacked on in our approach, but legitimately so by using the NN data as input to the nucleus-nucleus cascade. In any case one should again very much be cognizant of the small number of high  $p_{\perp}$  particles present in even central collisions at the highest RHIC energies. Some 5% – 10% of the integrated spectrum of mesons comes from  $p_{\perp} \geq 1$  GeV in an average NN event, and similar levels in  $Au + Au$ .

## VI. ACKNOWLEDGEMENTS

This manuscript has been authored under the US DOE grant NO. DE-AC02-98CH10886. One of the authors (SHK) is also grateful to the Alexander von Humboldt Foundation, Bonn, Germany and the Max-Planck Institute for Nuclear Physics, Heidelberg for continued support and hospitality. Useful discussion with the BRAHMS, PHENIX, PHOBOS and STAR collaborations are gratefully acknowledged, especially with C. Chasman, R. Debbé, F. Videbaek, D. Morrison, M. T. Tannenbaum, T. Ulrich and J. Dunlop.

- 
- [1] D. E. Kahana and S. H. Kahana, nucl-th/0406074; Phys. Rev. C **72**, 024903, (2005).
  - [2] I. Arsene *et al*, BRAHMS Collaboration, Phys. Rev. Lett., **91** 072305, (2003); R. Debbé, BRAHMS Collaboration nucl-ex/0403052; I. Arsene *et al*, the BRAHMS, nucl-ex/0307003; I. Arsene *et al*, the BRAHMS Collaboration, nucl-ex/0403050; I. Arsene *et al*, nucl-ex/0307003.
  - [3] B. B. Back *et al*, PHOBOS Collaboration, Phys. Lett., **461**, 297, (2004); B. B. Back *et al*; B. B. Back *et al*, the PHOBOS Collaboration, Phys. Rev. Lett., **91** 072302-1, (2003).
  - [4] S. S Adler *et al*, PHENIX Collaboration, Phys. Rev. C. **69**, 034910, (2004); Phys. Rev. Lett. **91**, 072301, 2003; K. Adcox *et al*, nucl-ex/0207009.
  - [5] C. Adler *et al*, STAR Collaboration, Phys. Rev. Lett. **91**, 172302, 2003; Phys. Rev. Lett. **89**, 202301, (2002); J. Adams *et al*, Phys. Rev. Lett. **91** 172302, 2005.
  - [6] D. E. Kahana and S. H. Kahana, *Proceedings, RHIC Summer Study'96*, 175-192, BNL, July 8-19, 1996; D. E. Kahana and S. H. Kahana, Phys. Rev. C **58**, 3574 (1998); Phys. Rev. C **59**, 1651 (1999).
  - [7] D. E. Kahana, S. H. Kahana, Phys. Rev. C **63**, 031901 (2001).
  - [8] Proc. International Conference on the Physics of the Quark-Gluon Plasma, Ecole Polytechnique, Palaiseau, France, Sept. 4-7, 2001; D. E. Kahana, S. H. Kahana, nucl-th/0208063.
  - [9] H. Stoecker and W. Greiner, Phys. Rep. **137**, 277 (1986; R. Mantiello, A. Jahns, H. Sorge and W. Greiner, Phys. Rev. Lett., **74**, 2180 (1995).
  - [10] H. Sorge, Phys. Rev. C **52**, 3291 (1995).
  - [11] S. A. Bass *et al*, Nucl. Phys. A **661**, 205 (1999).
  - [12] B. Andersson, G. Gustafson, G. Ingelman, and T. Sjostrand, Phys. Rep **97**, 31 (1983); B. Andersson, G. Gustafson, and B. Nilsson-Almqvist, Nucl. Phys B **281**, 289 (1987).

- [13] A. Capella and J. Tran Van, Phys. Lett. **B93**, 146 (1980) and Nucl. Phys. **A461**, 501c (1987); A. Capella *et al.*, nucl-th/0405067 and hep-ph/0403081.
- [14] K. Werner, Z. Phys. **C42**, 85 (1989); K. Werner, J. Aichelin, Phys. Rev. Lett. **76** (1996) 1027-1030; H. J. Drescher, M. Hladik, S. Ostapchenko, K. Werner, Proc. of the "Workshop on Nuclear Matter in Different Phases and Transitions", Les Houches, France, March 31 - April 10, 1998; K. Werner Invited lecture, given at the Pan-American Advanced Study Institute "New States of Matter in Hadronic Interactions" Campos de Jordao, Brazil, January 7-18, 2002, hep-ph/0206111.
- [15] B. Zhang, C. M. Ko, B.-A. Li, Z. Lin, nucl-th/9904075; Z. Lin and C. M. Ko, Phys. Rev. **C68**, 054904 (2003); Z. Lin *et al.* Nucl. Phys. **A 698**, 375-378 (2002).
- [16] J. Ranft and S. Ritter, Z. Phys. **C27**, 413 (1985); J. Ranft Nucl. Phys. **A498**, 111c (1989).
- [17] D. Boal, *Proceedings of the RHIC Workshop I*, (1985) and Phys. Rev. **C33**, 2206 (1986).
- [18] K. J. Eskola, K. Kajantie and J. Lindfors, Nucl. Phys. **B323**, 37 (1989).
- [19] X. -N. Wang and M. Gyulassy, Phys. Rev. **D44**, 3501 (1991); X. -N. Wang, nucl-th/000814 and nucl-th/0405029; X. -N. Wang hep-ph/0405125.
- [20] M. Gyulassy and X. N. Wang, Comp. Phys. Comm. **83**, 307 (1994),
- [21] K. Geiger and B. Mueller Nucl. Phys. **B369**, 600 (1992); K. Geiger Phys. Rev. **D46**, 4965 and 4986 (1992); K. Geiger, *Proceedings of Quark Matter'83*, Nucl. Phys. **A 418**, 257c (1984); K. Geiger, Phys. Rev. **D 51**, 2345 (1995).
- [22] S. A. Bass, B. Mueller and D. K. Srivastava, Phys. Rev. Lett. **B 551**, 277 (2003); S. A. Bass *et al.*, Nucl. Phys. **A661**, 205 (1999).
- [23] K. Gallmeister, C. Greiner and Z. Xu, Phys. Rev. **C67**, 044905 (2003).
- [24] W. Cassing, K. Gallmeister, C. Greiner Nucl. Phys. **A735**, 277-299 (20004); J. Geiss, C. Greiner, E. Bratkovskaya, and U. Mosel, Phys. Lett. **B447**, 31 (1999).
- [25] L. V. Gribov, E. M. Levin and M. G. Ryskin, Phys. Rep. **100**, 1 (1983); Nucl. Phys. **B188**, 555 (1981); A. H. Mueller and J. Qiu, Nucl. Phys. **B268**, 427 (1986); E. M. Levin and M. G. Ryskin, Phys. Rep. **189**, 267 (1990).
- [26] L. McLerran and R. Venugopalan, Phys. Rev. **D49**, 2223 (1994); Phys. Rev. **D59**, 094002 (1999); D. Kharzeev, E. Levin and L. McLerran, Phys. Lett. **B561**, 93 (2003).
- [27] D. Kharzeev, E. M. Levin and L. McLerran hep-ph/0210332 (2002); L. McLerran hep-ph/0402137 (2004); D. Kharzeev, E. M. Levin and L. McLerran, hep-ph/0403271 (2004).
- [28] K. Goulianos, *Phys. Rep.* **101**, 169 (1983).
- [29] G. Eksping for the UA5 Collaboration, Nucl. Phys. **A461**, 145c (1987); G. J. Alner for the UA5 Collaboration, Nucl. Phys. **B291**, 445 (1987).
- [30] C. Albajar *et al.*, the UA1 Collaboration, Nucl. Phys. **B335**, 261-287 (1990).
- [31] Y. Eisenberg *et al.*, Nucl. Phys. **A461**, 145c (1987) G. J. Alner *et al.*, Nucl. Phys. **B 291**, 445 (1987); F. Abe *et al.*, Phys. Rev. **D41** 2330, (1990).
- [32] B. B. Back *et al.*, the PHOBOS Collaboration, Phys. Rev. Lett. **88**, 22302 (2002).
- [33] J. W. Cronin *et al.*, Phys. Rev. **D91**, 3105 (1979).
- [34] B. Z. Kopeliovich *et al.*, hep-/030120, Nucl. Phys. **A** (in press).
- [35] A. H. Mueller, Eur. Phys. J. **A1**, 19 (1998).
- [36] E. V. Shuryak and I. Zahed, hep-ph/0307267; and hep-th/0308073.
- [37] S. Datta, F. Karsch, P. Petreczky and I. Wetzorke, hep-lat/0208012; hep-lat/0403017; hep-lat/0309012.
- [38] D. Molnar and M. Gyulassy, nucl-th/0102031; nucl-th/0104018; D. Molnar, presentation at workshop on "Creation and Flow of Baryons in Hadronic and Nuclear Collisions", ECT, Trento, Italy, May 3-7, 2004 (unpublished).
- [39] S. S. Adler *et al.*, the PHENIX Collaboration, Phys. Rev. Lett. **91**, 182301 (2003); C. Adler *et al.*, the STAR Collaboration, Phys. Rev. Lett. **87**, 182301 (2001), S. Manly, the PHOBOS Collaboration, Proceedings of the 20th Winter workshop on Nuclear Dynamics, Trelawney Beach, Jamaica, March 15-20, 2003.
- [40] K. Gottfried, Phys. Rev. Lett. **32**, 957 (1974); and Acta. Phys. Pol **B3**, 769 (1972).
- [41] S. S. Adler *et al.*, PHENIX Collaboration, Phys. Rev. Lett. **91** 241803, (2003).
- [42] I. L. Arsene *et al.*, BRAHMS Collaboration, nuc-ex/0403050, (2004).
- [43] K. Adcock *et al.*, PHENIX Collaboration, nucl-ex/0207009.
- [44] M. Shimamura, for the PHENIX Collaboration, nucl-ex/0510023.



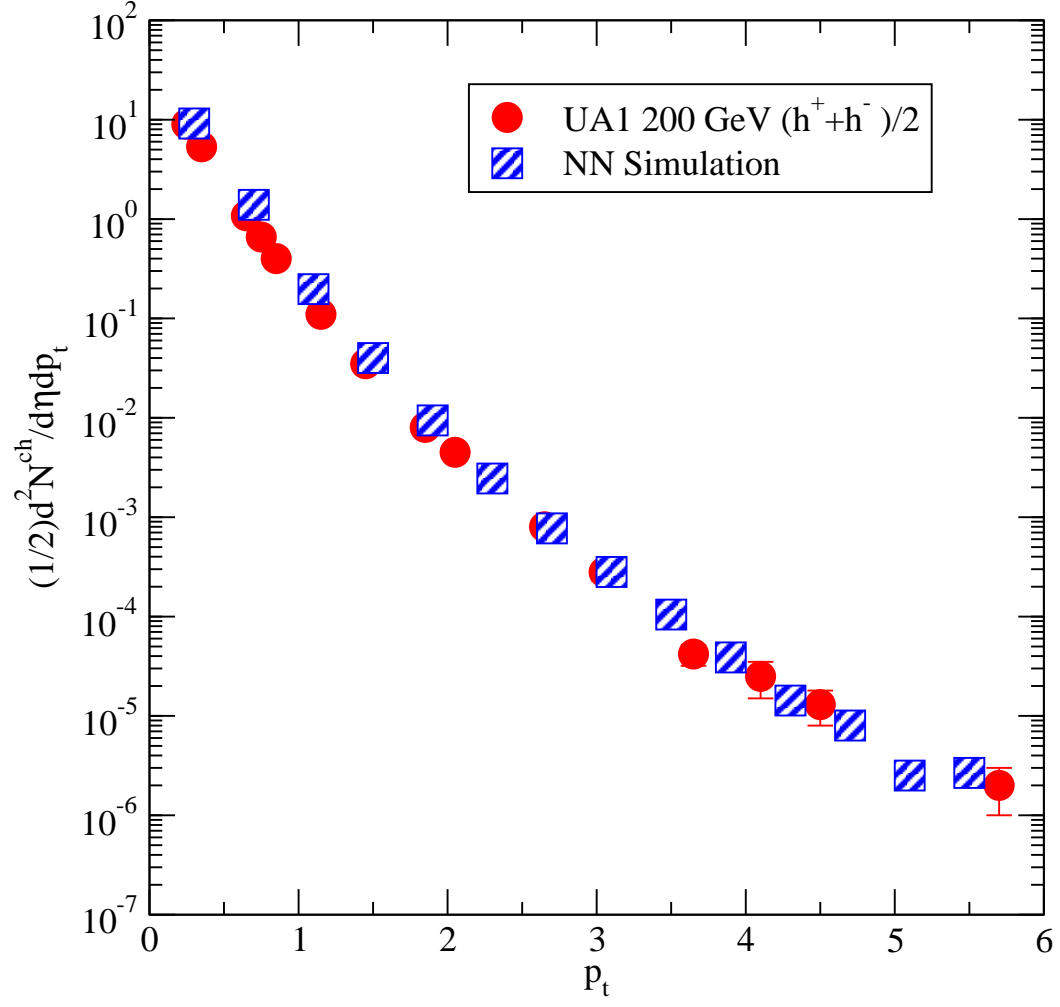


FIG. 1: PP Pseudorapidity spectra: Comparison of UA1 minimum bias 200 GeV NSD data [30] with an appropriate LUCIFER simulation. The latter is properly obtained from experiment and an input to the ensuing AA collisions; thus does not constitute a ‘set’ of free parameters.

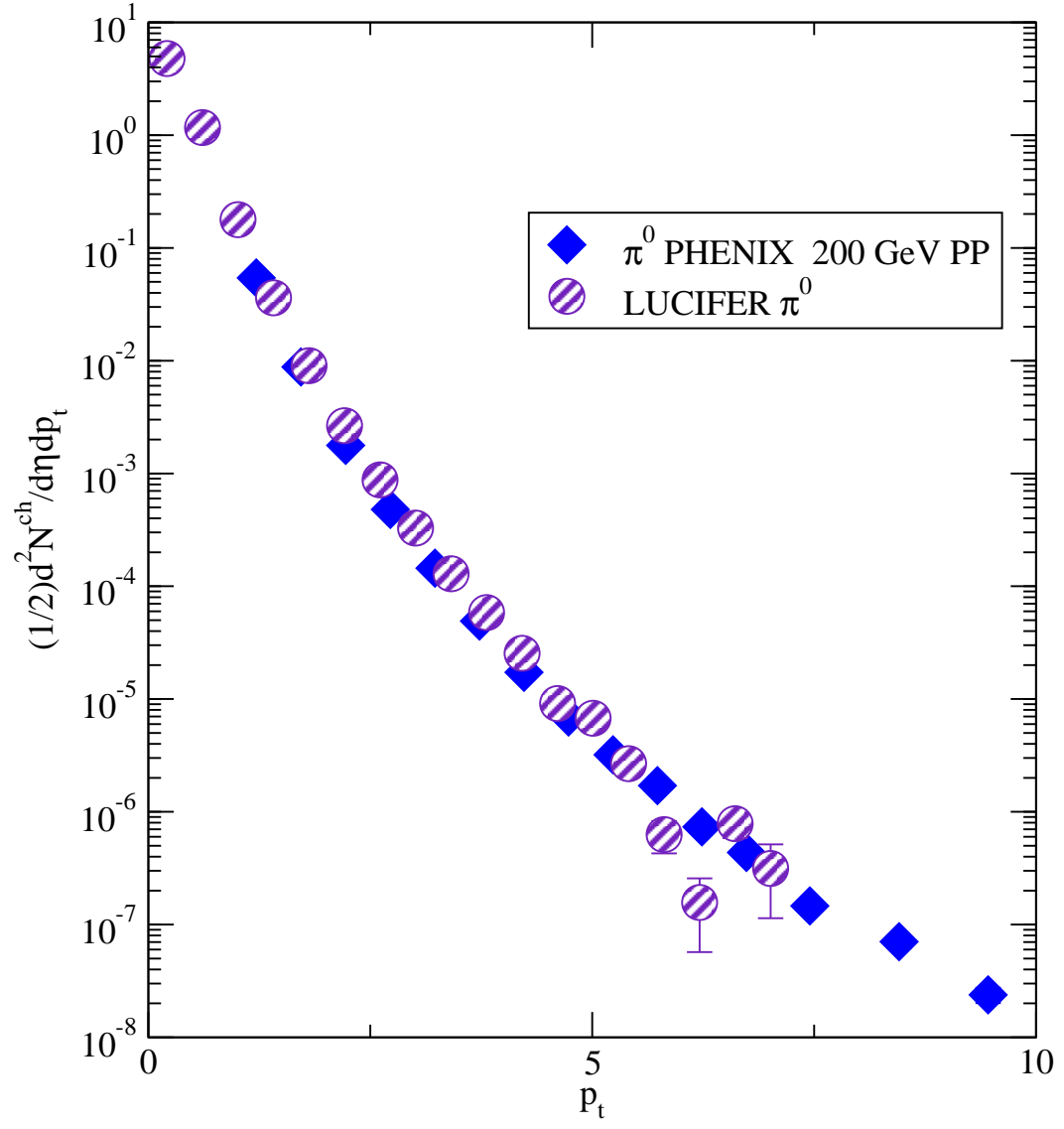


FIG. 2: A similar transverse momentum  $\pi^0$  spectrum from PHENIX PP [41] vs simulation.

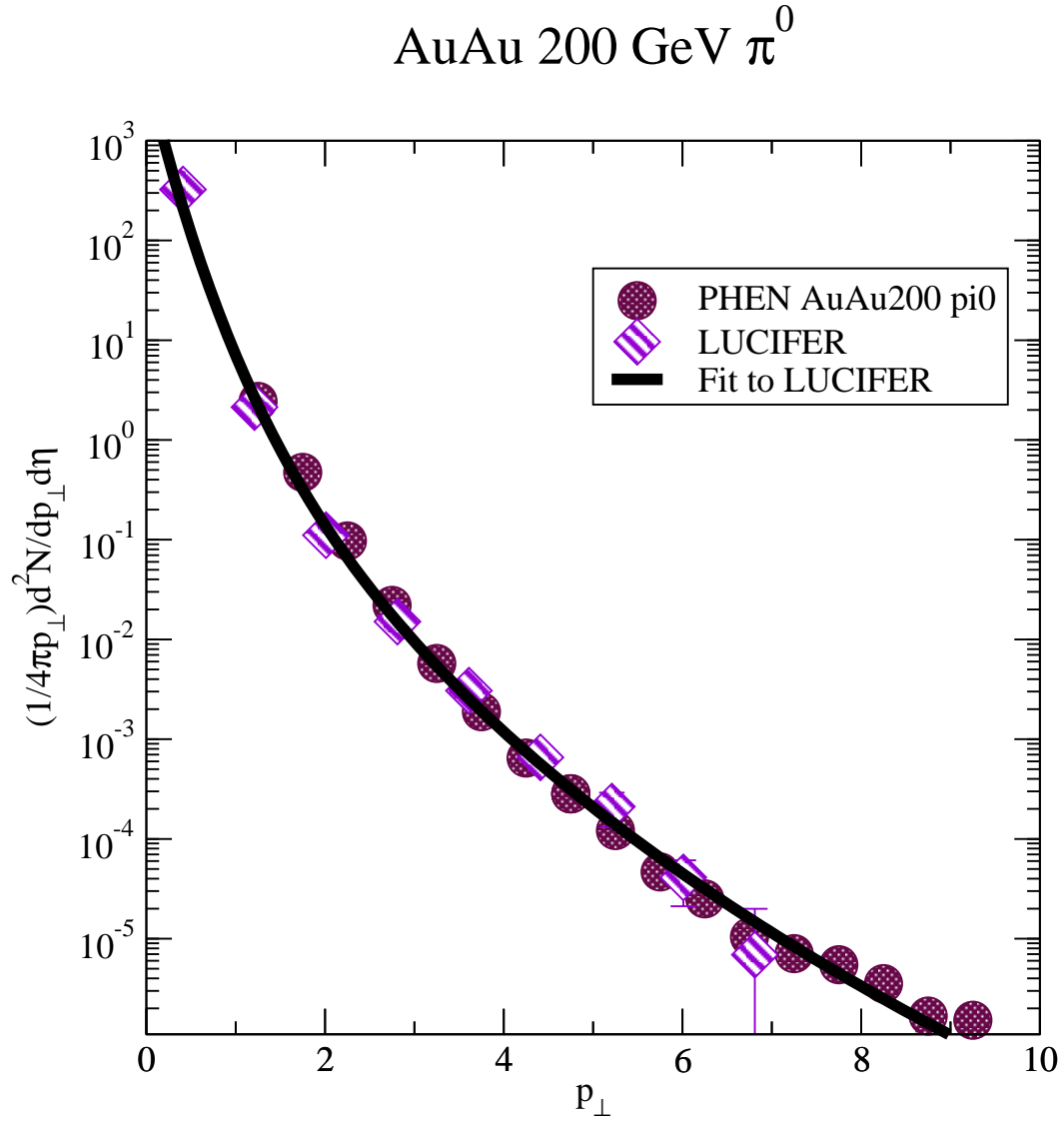


FIG. 3: Central PHENIX  $\pi^0$  200 GeV for Au+Au vs simulation. Curves for different choices of the production time  $\tau_p$ , say 0.02 fm/c and 0.04 fm/c differ very little, since in effect the cascade effectively begins somewhat later, near 0.25 – 0.35 fm/c and continues much longer to tens of fm/c. Centrality for PHENIX is here 0% – 10%, roughly for impact parameters  $b < 4.25$  fm. in the simulation.

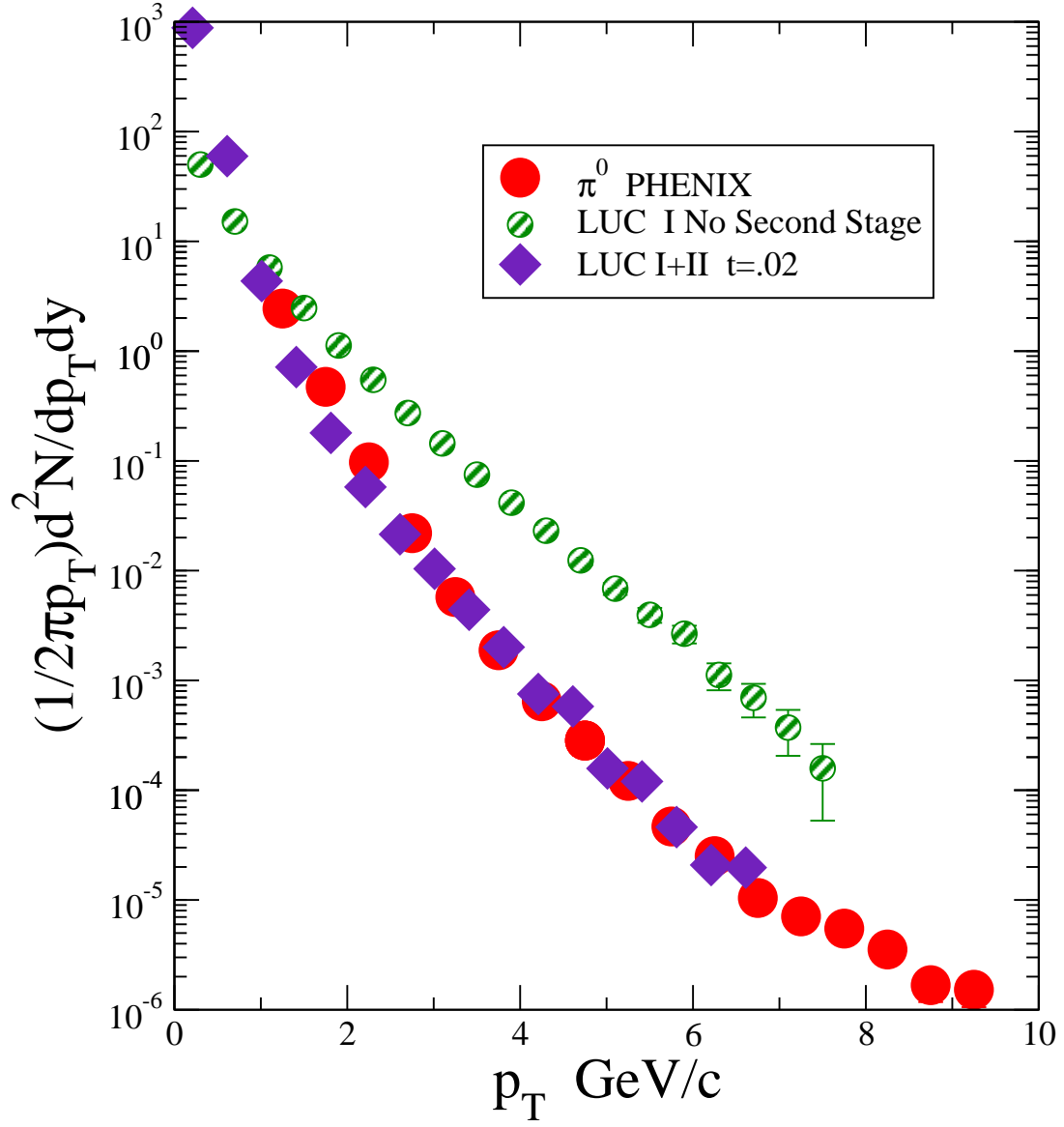


FIG. 4: The  $\pi^0$  transverse momenta yields for stage I, no final cascade, vs those for the full stage I+II calculation. Clearly there is considerable suppression in the final cascade. Recalling that the experimentalists quote a ‘direct’ suppression of  $\sim 4$ – $5$  for the ratio in Eqn.(1) at the highest  $p_\perp$ , there is at the end of I an enhancement  $\sim 3$ , *i. e.* still a Cronin effect in this first stage.

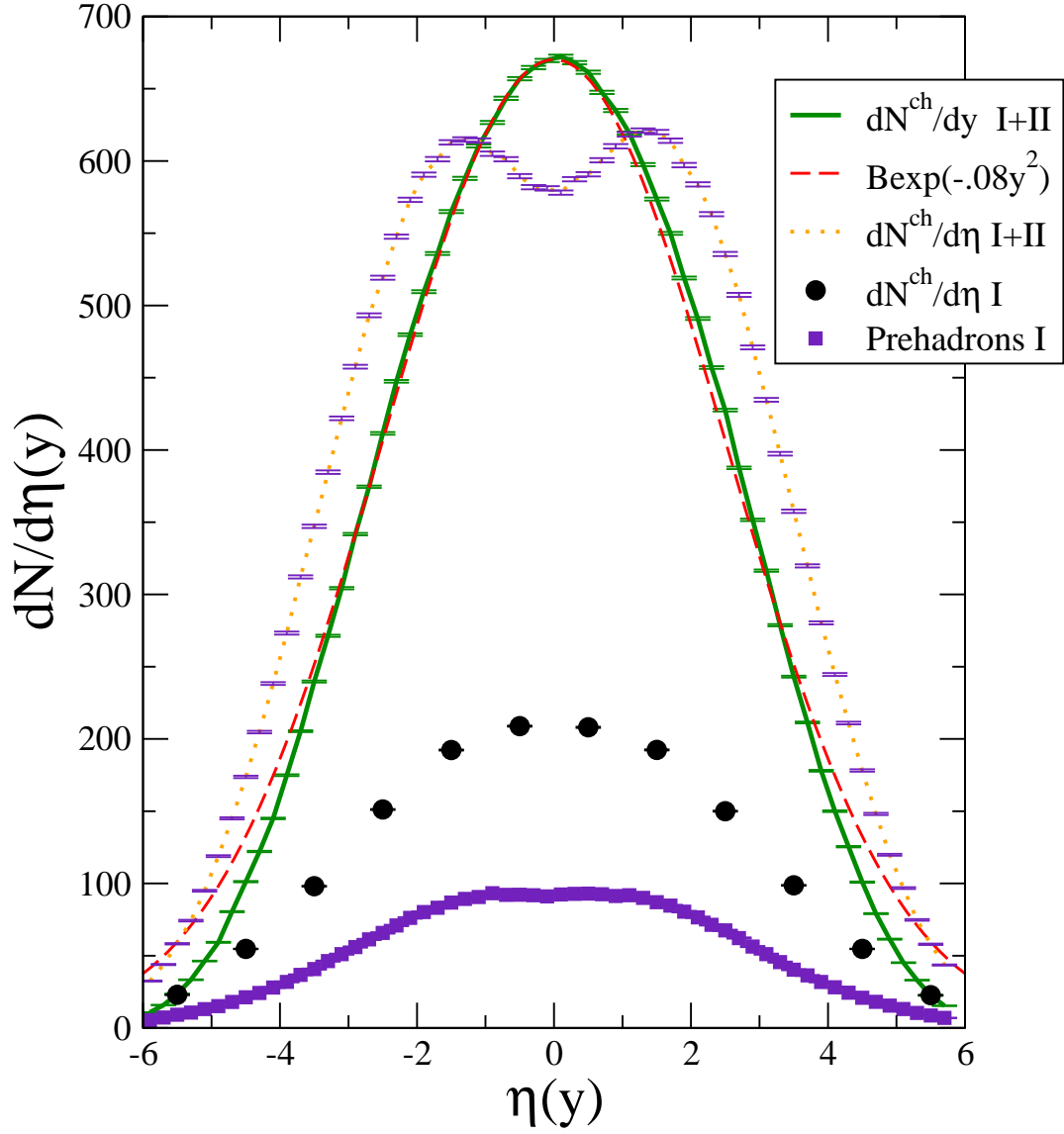


FIG. 5: Pseudorapidity and rapidity spectra for charged mesons and prehadrons at various stages of the collision simulation. The gaussian fit to the charged pion rapidity distribution approximates preliminary BRAHMS [42] results, certainly in its FWHM, and hence demonstrates the validity of the simulation (solid line) for  $dN^{ch}/dy$ . The successive retreats, first to phase I of the simulation and then to only prehadrons in phase I, *i. e.* no decays, indicates both the reduction in cascading participants and in the fraction of  $E_{\perp}$  available at the earliest moments of the cascade.

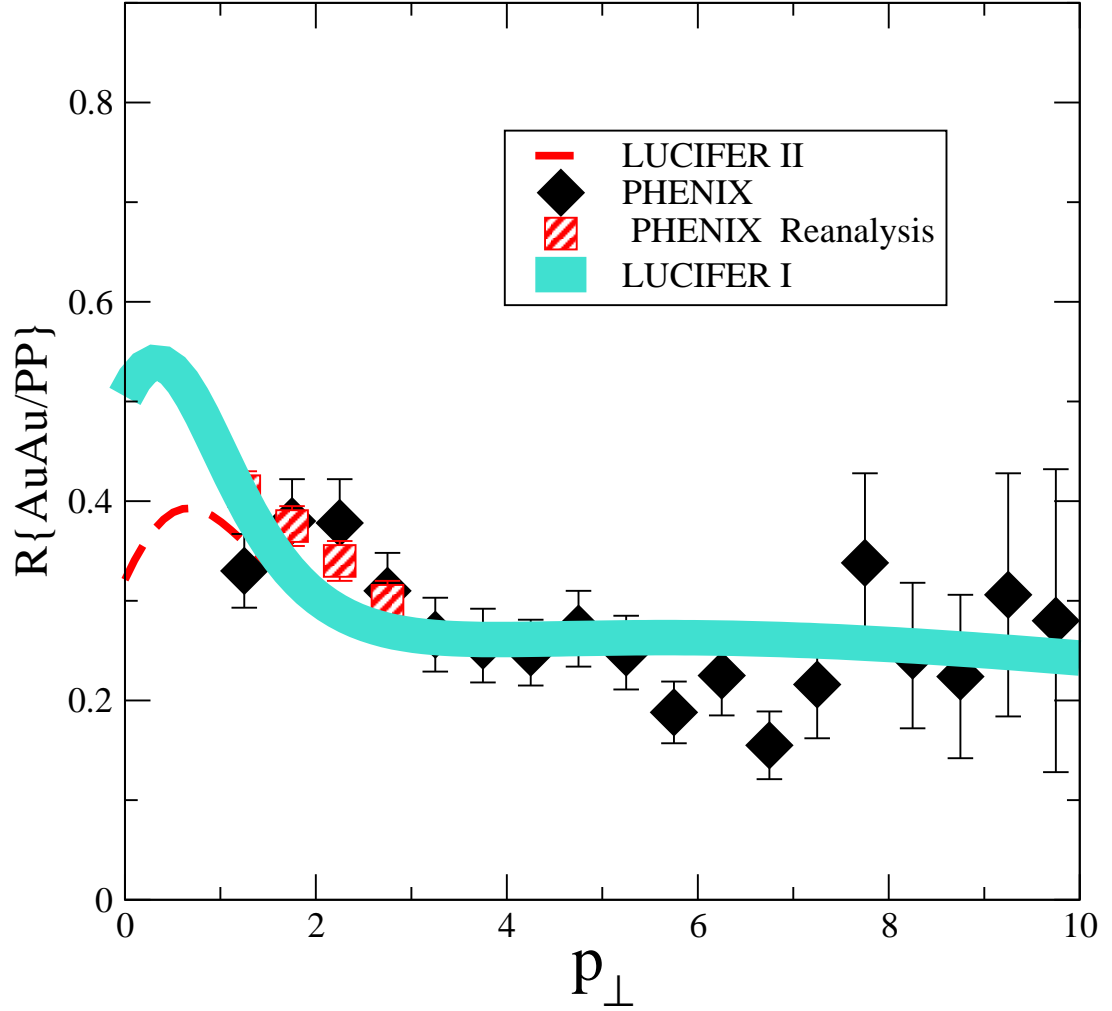


FIG. 6:  $R_{AuAu/NN}$ : Ratio of  $\pi^0$  production in  $Au + Au$  collisions to that in NN at  $\sqrt{s} = 200$  GeV for 0% – 10% centrality. The binary collision number selected at this centrality is  $N_{coll}=950$ , while the divisor for both PHENIX and LUCIFER curves shown here is one fit to the PHENIX PP data shown in Fig.(7). The resultant ratio is especially sensitive to the PHENIX NN data. LUCIFER curves are shown for two choices differing not in the  $Au + Au$  calculations but only in the fitted PHENIX extrapolation to lowest  $p_{\perp}$ , where of course there is no data. The extra points for the PHENIX ratio at the four lowest  $p_{\perp}$  GeV/c are from more recent analysis [44]. Thus the general shape and magnitude of the simulation conforms well with this most recent data analysis, both exhibiting a rise towards smaller  $p_{\perp}$ . This feature is also present in the very similar 0% – 5% measurement [44]. The calculated suppression is somewhat excessive at low  $p_{\perp}$ .

PP 200 GeV

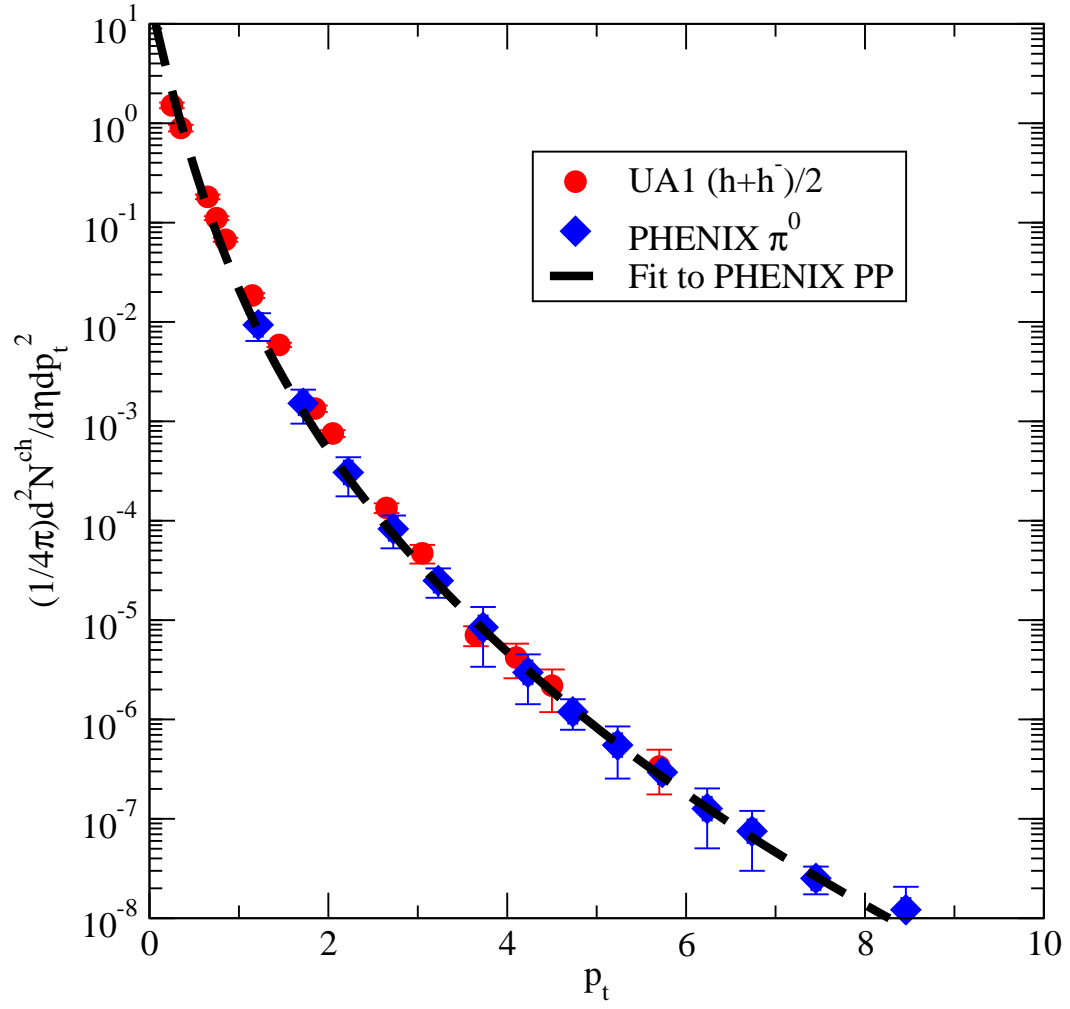


FIG. 7: PHENIX  $\pi^0$  200 GeV/c for NN: The fit to the PHENIX PP data used in the ratios shown in Fig.(6) is shown against the observations.